JOURNAL OF THE KOREAN ASTRONOMICAL SOCIETY
41: 65 ~ 76, 2008 June

VERTICAL PROPERTIES OF THE GLOBAL HAZE ON TITAN DEDUCED FROM METHANE BAND SPECTROSCOPY BETWEEN 7100 AND 9200Å

CHAE KYUNG SIM[1], SANG JOON KIM[1], JOO HYEON KIM[1], HAING JA SEO[1], AERAN JUNG[1], AND JI HYUN KIM[2]
[1]Department of Astronomy and Space Science, Kyung Hee University, Yongin, 446-701, Korea
E-mail: sjkim1@khu.ac.kr
[2]Department of Astronomy, Boston University, Boston, MA02215, U.S.A.
(Received February 28, 2008; Accepted June 24, 2008)

ABSTRACT

We have investigated the optical properties of the global haze on Titan from spectra recorded between 7100 and 9200Å, where CH_4 absorption bands of various intensities occur. The Titan spectra were obtained on Feb. 23, 2005 (UT), near the times of the Cassini T3 flyby and Huygens probe, using an optical echelle spectrograph (BOES) on the 1.8-m telescope at Bohyunsan Observatory in Korea. In order to derive the optical properties of the haze as a function of altitude, we developed an inversion radiative-transfer program using an atmospheric model of Titan and laboratory CH_4 absorption coefficients available from the literature. The derived extinction coefficients of the haze increase toward the surface, and the coefficients at shorter wavelengths are greater than those at longer wavelengths for the 30 – 120 km altitude range, indicating that the Titanian haze becomes optically thin toward the longer wavelength range. Total optical depths of the haze are estimated to be 1.4 and 1.2 for the 7270 – 7360Å and 8940 – 9150Å ranges, respectively. Based on the Huygens/DISR data set, Tomasko et al. (2005) reported total optical depths of 2.5 – 3.5 at 8290Å, depending on the assumed fractal aggregate particle model. The total optical depths based on our results are smaller than those of Tomasko et al., but they partially overlap with their results if we consider a large uncertainty from possible variations of the CH_4 mixing ratio over Titan's disk. We also derived the single scattering albedo of the haze particles as a function of altitude: it is less than 0.5 at altitudes higher than ~150 km, and approaches 1.0 toward the surface. This behavior suggests that, at altitudes above ~150 km, the average particle radius is smaller than the wavelengths, whereas near the surface, it becomes comparable or greater.

Key words : Titan:atmosphere — Titan:haze — visible range — spectroscopy

I. INTRODUCTION

The recent historic probe of Titan by CassiniHuygens during its descent from the high altitude atmosphere to the surface has provided many important discoveries and new insights on the properties of the atmosphere and the surface of Titan (e.g., Tomasko et al. 2005; Niemann et al. 2005, Fulchignoni et al., 2005), which have been shrouded by thick haze. Since the Huygens probe was able to investigate only the landing site during the descent, the global average of the altitudinal distributions of haze has not been investigated.

The global scale distributions of haze have been investigated mainly from ground observatories (McKay et al. 1989; Rannou et al. 1995; Anderson et al. 2004; Negrão et al., 2006 and earlier works referred therein) or from Hubble Space Telescope (HST) (Young et al. 2002); and, of course, the Visual and Infrared Mapping Spectrometer (VIMS) on Cassini spacecraft have recently provided the spectro-imagery of Titan, and detailed analyses for the global haze distribution are now underway (e.g., McCord et al. 2006).

Over the wavelength range of 7100 and 9200Å, the Titan's surface can be glimpsed between CH_4 absorptions through the thick haze layers (e.g., Smith et al. 1996), while in the wavelength range shorter than 7000Å the Titan's atmosphere becomes optically thick due to Mie scatterings by haze particle aggregates and Rayleigh scatterings by molecules in the atmosphere (e.g., McKay et al. 1989). The CH_4 absorption bands between 7100 and 9200Å are useful to investigate haze opacities at various altitudes, because the peaks of contribution functions occur at different altitudes (Kim et al., 2005). There is another useful wavelength range at 1.0–3.0 μm, where CH_4 has several ro-vibrational bands with contribution functions occurring at different altitudes; consequently, this near-IR range has been targeted for intense investigations of surface, haze, and clouds for more than a decade (e.g., Griffith, Owen, and Wagener, 1991; Coustenis et al. 1995; Griffith et al. 2003; Negrão et al. 2006). However, the near-IR range, the 7100 and 9200Å range, unlike the near-IR range,

Corresponding Author: S. J. Kim

is almost free from the influence of other molecular bands, and easily accessible from low-altitude ground observatories without significant telluric absorptions (Karkoschka, 1994).

We obtained high-resolution spectra of Titan between 7100 and 9200Å using an echelle spectrograph on the 1.8-m telescope at Bohyunsan Observatory in Korea on Feb. 23, 2005 (UT) near the T3 flyby of Cassini on Feb. 15, 2005, and the entry of Huygens probe on Jan. 15, 2005. We developed an inversion program, using a modified radiative-transfer code of Kim et al. (2005) in order to derive the vertical variations of global haze properties from the spectra. Our investigation on the opacities of the globally distributed haze differs from previous investigations in the following aspects —

Rages and Pollack (1983) derived vertical properties of haze in Titan's upper atmosphere down to 100 km altitude from high-phase angle images from Voyager 2, whereas our spectral range, 7100−9200Å, is sensitive mainly to an altitude range below 200 km. McKay et al. (1989) constructed a radiative-convective model for the thermal structure of Titan's atmosphere which is largely a theoretical work focusing on the thermal balance of the atmosphere. They presented a vertical distribution of the haze using spherical particle models based on a low-resolution spectrum of Neff et al. (1984), and CH_4 absorption coefficients at 95 K estimated by Pollack et al. (1986). Pollack et al. derived their result from CH_4 coefficients measured at a room temperature utilizing liquid CH_4 absorption coefficients measured at 95 K assuming a similar spectral behavior between CH_4 gas and liquid. This assumption is, however, highly uncertain; and instead of their data, we used CH_4 absorption coefficients of O'Brien and Cao (2002), and Singh and O'Brien (1995) measured at 77 K, along with CH_4 absorption coefficients deduced from planetary spectra by Karkoschka (1994), as described in §3.1 in detail. Rannou et al. (1995) used a fractal model for the haze particles, and derived a vertical distribution of the haze using the spectrum of Neff et al. (1984) and the same CH_4 absorption coefficients of McKay et al. (1989), which is uncertain, as just mentioned.

Young et al. (2002) took 6 images between 8880 and 9530Å using the WFPC2 (Wide Field Planetary Camera 2) on HST, from which the Titan disk was resolved, an advantage for limb darkening analyses. Although able to derive latitudinal and vertical distributions of haze opacities, they used narrow band filters with 1−2 % spectral resolution, which is lower than ours (e.g. 0.25% at 8000Å), and their wavelength coverage did not extend to our shorter wavelength range of 7100−8880Å. Anderson et al. (2004) obtained narrow-band images near 9400Å at the Mount Wilson 2.54-m telescope and derived extinction of haze as a function of altitude. Because the wavelength range near 9400Å is almost free from the CH_4 absorptions, their data are useful to probe haze properties near the surface. Consequently, their contribution function that can probe atmospheric altitude range is considerably limited compared to our much wider 7100−9200Å wavelength range. Their results, however, contain large error bars, significantly deviated from the results of other works.

Recently, Tomasko et al. (2005) presented haze extinction optical depths at 5310, 8290, and 15000Å, as a function of altitude derived from Huygens/DISR (Descent ImagerSpectral Radiometer) data. Their 8290Å result is interesting to compare with our result and a comparison with ours is described in §3.4. Hirtzig et al. (2005) used CFHT(Canada-France-Hawaii Telescope)/OASIS(Adaptive Optics Spectro-Imaging System) to obtain spectro-imagery between 8600−10200Å whose main purpose was to derive the albedos of Titan.

II. OBSERVATIONS AND DATA REDUCTIONS

We observed Titan on Feb. 23, 2005 (UT) using a fiber-fed echelle spectrograph (BOES) on the 1.8-m telescope at Bohyunsan Observatory in Korea over the 3800 ∼ 10200Å wavelength range with a spectral resolving power of 30,000 ($\Delta\lambda \sim 0.27\mathring{A}$). Our resolution is the highest among previous Titan observations in the 7100 - 9200Å range. The raw Titan spectra contain telluric as well as solar absorption and emission lines. We used Kitt Peak solar atlases (e.g., Hinkle et al. 2003) obtained from the Digital Library of the National Solar Observatory (http://diglib.nso.edu) to remove the solar lines effectively. Since the spectral resolution of Kitt peak solar spectrum is higher than the BOES resolution, the Kitt peak spectrum has been convolved with the BOES resolution. The seeing of the night sky on the observing date was slightly greater than 1″, and the field-of-view was 4.2″, enough to fill the whole disk of Titan, which was 0.8″ at the times of the observations. We also took the spectra of the Moon, which were used to remove telluric absorption lines in the Titan spectra. For wavelength calibration, we considered a Doppler shift (e.g. $\Delta\lambda = 0.53$Å at 8000Å) caused by a relative velocity of -19.63 km/s between Earth and Titan on the observing date. Data reductions were carried out using image-processing software, IRAF and IDL.

The shorter wavelength range less than 7100Å is strongly influenced by Mie scatterings by haze particle aggregates and Rayleigh scatterings by nitrogen molecules (e.g., McKay et al. 1989; Young et al. 2002), and the CH_4 absorptions become significantly weak. The longer wavelength range of the BOES spectrum greater than 9200Å becomes noisy due to low sensitivities of the BOES instrument. We, therefore, chose the 7100 - 9200Å range for the purpose of investigating the optical properties of haze layers. We present an example of a segment of the BOES spectrum in Fig. 1 along with a laboratory spectrum of O'Brien and Cao (2002) for comparison, which will be described in detail in §3.2.

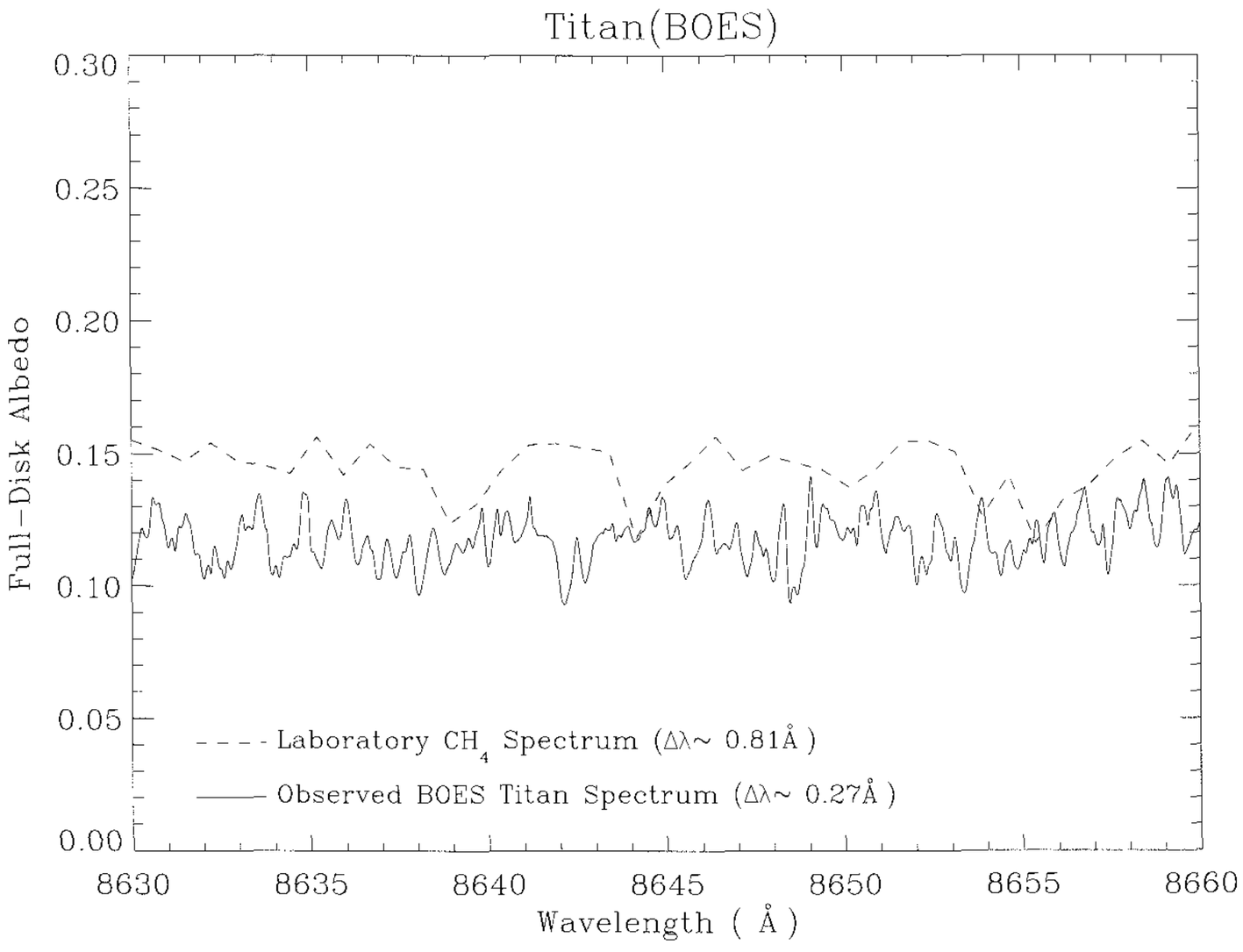

Fig. 1.— An example of a segment of the BOES spectrum of Titan compared with a laboratory CH_4 spectrum of O'Brien and Cao (2002). The spectral resolutions of the BOES and the laboratory spectra are 0.27 and 0.81Å, respectively. The intensities of the laboratory spectrum are set in an arbitrary scale to be compared with the BOES spectrum. The BOES spectrum with a 0.27Å resolution shows many absorptions features, which is considered to be mostly due to CH_4. We are, however, unable to confirm that all of these absorption features are due to CH_4 because of lack of similar high-resolution laboratory spectra available in the literature. Obviously, we need high-resolution laboratory CH_4 spectra measured at the atmospheric temperatures of Titan in order to accurately model the Titan spectra.

Since our high-resolution spectra are extracted from many different orders, the derivations of absolute intensities are not accurate, although we used the Moon spectra for absolute calibration. This difficulty has been well known for high-resolution spectroscopy, since Hall et al. (1994) and Škoda and Hensberge (2003) described this problem of merging spectral orders from a fiber-fed echelle spectrograph. Therefore, we adopted a full-disk albedo spectrum listed in Table III of Karkoschka (1994) for intensity scale. The relative fit between the albedo spectrum of Karkoschka and our BOES spectrum is, however, excellent. It should be noted that the full-disk albedo of Karkoschka at the times of their observations on July 25, 1993 (UT) was very close to the geometric albedo of Titan, though not exactly same. The illuminated fractions of the Titan disk at the times of their and our observations were 99.946 and 99.862%, respectively. The resultant albedo spectrum has been binned with a 20Å box function (Fig. 2) to derive haze opacities, which is supposed to vary smoothly with wavelengths; besides, high signal-to-noise ratio data are needed in order to retrieve good quality haze opacities from the observations. The reduced high-resolution spectra as well as the binned spectrum are available to the planetary community at an internet site: http://padra.khu.ac.kr.

An issue on a possible significant change in the Titan's brightness between the 1993 observ ations of Karkoschka and our 2005 observations can be resolved with an investigation carried out by Lorenz et al. (1999). According to Lorenz et al., the seasonal brightness change of Titan can be up to ± 10%, but the difference in the brightness between 1993 and 2005 is estimated to be approximately 2.4%, which is not large enough to influence our results. Finally, this uncertainty along with other uncertainties discussed in §3.4 is summarized in Table 1, together the final error bars of the derived haze opacities have been determined.

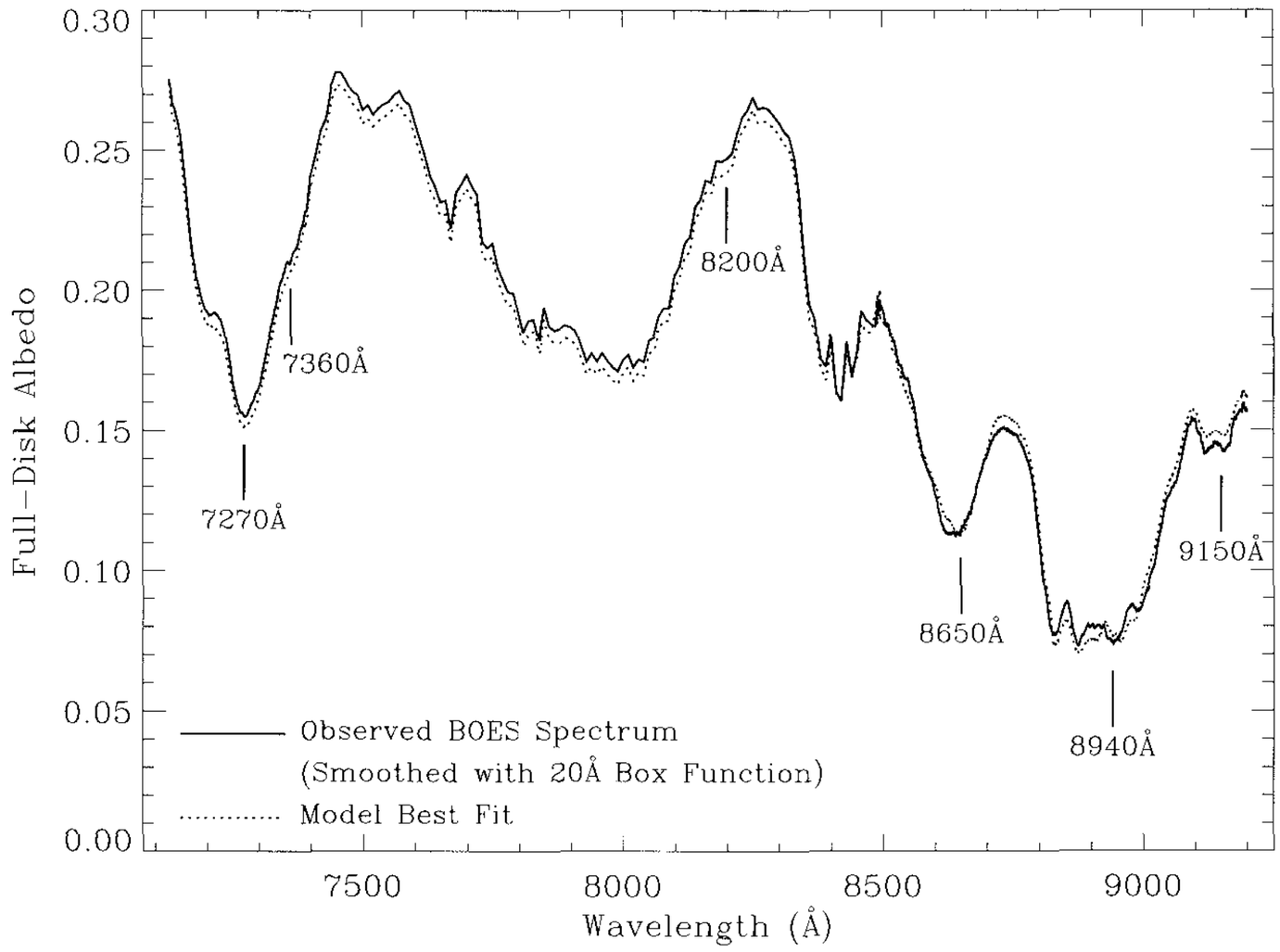

Fig. 2.— The smoothed BOES spectrum (solid line) with a 20Å box function; and the best fit model spectrum (dotted line). The iterations of the inversion program were stopped, when the differences between the BOES and model spectra became less than an observational error bar of 0.005 in the albedo scale.

III. RADIATIVE TRANSFER CALCULATIONS

(a) Models for the Atmosphere, Clouds, and Surface Albedos

We adopted a radiative transfer model developed by Kim et al. (2005) who used it for the construction of 3-micron synthetic spectra of Titan. This model uses a 2-stream approximation and includes the absorptions and scatterings of haze particles, as well as absorptions and emissions of atmospheric molecules and molecules. For the scatterings of haze particles, Kim et al. used single-scattering approximations, which are the integrations of istotropically-scattered lights in all directions (e.g., Eq. 1.2.4 in Chamberlain and Hunten, 1987). We modified the program adding Rayleigh scatterings by molecules, and developed an inversion program using the same approximations as described in §3.3 in detail. The major reason for using these approximations is that we are unable to derive unique solutions for all the quantities describing the physical nature of haze particles, such as the index of refraction, scattering phase function, and size and shape distributions from the BOES spectrum, because of excessive number of free parameters to be retrieved. Therefore, we have designed the inversion program to derive only obtainable quantities, which are extinction coefficients and, if possible, single scattering albedos as a function of wavelength and altitude. The uncertainty arising from using the single-scattering approximations instead of multiple scatterings as well as the uncertainty from the 2-stream approximation will be discussed in §3.4.

The atmospheric model contains 81 plane-parallel layers from the surface up to a pressure level of 10^{10} bar. We, however, mostly used 33 layers from the surface up to ~300 km, since this altitude range mainly influences the spectral range between 7100 and 9200Å. The spherical geometry of Titan was considered for the calculation of global radiation from the Titan disk. A temperature-pressure (T-P) profile for the troposphere and stratosphere was adopted from a recent result from the Huygens Atmospheric Structure Instrument (HASI) (Fulchignoni et al. 2005; Harri et al. 2006). The T-P profile was measured from the Huygens landing site, which could be different in other locations. The HASI result is, however, remarkably similar to the Voyager radio occultation result of Lindal et al. (1983). The Voyager IRIS (Infrared Interferometer Spectrometer) measurements of brightness temperatures indicate that the global temperature variation is less than a few degrees in the troposphere and in the

low stratosphere, and the Voyager IRIS team (Flasar et al. 1981) recognized that radiative response times below the 10 mbar level are equal or longer than the Saturnian year. The temperature-dependence of the CH_4 molecular bands in the visible range has been reported by Karkoschka (1998), O'Brien and Cao (2002), and Bowles et al. (2006), but the temperature-dependency of these CH_4 molecular bands seems to be significantly weaker than that of typical ro-vibrational bands in infrared ranges. We expect that the use of the HASI T-P result should not cause significant uncertainty for the construction of a globally representing CH_4 absorption features between 7100 and 9200Å.

One of the important confirmations of the Cassini/Huygens mission is that CH_4 in the Titan's atmosphere plays the same role as H_2O in the Earth's atmosphere. Its mixing ratio, therefore, may vary depending upon the weather on the surface of Titan. Paulo and Griffith (2006) suggested possible global variations of the CH_4 mixing ratios up to a factor of 2 based on the variation of CH_4 absorption depths in the VIMS spectro-imagery of Titan. For our radiative transfer calculations, we adopted the CH_4 mixing ratios from the GCMS (Gas Chromatograph Mass Spectrometer)/Huygens (Niemann et al. 2005). A factor of 2 uncertainty in the global mixing ratio is considered in our calculations of error bars for the retrieved optical properties of haze.

The brightness of Titan should be affected by possible transient clouds, which usually occur in the south polar region and occasionally in the equatorial region (Griffith et al., 1998). Unfortunately, we could not find infrared images taken from Earth on Feb. 23, 2005 (UT). Gendron et al. (2005) took 2.12-m Titan images on Jan. 14−16, 2005 with the ESO's Very Large Telescope (VLT) showing no significant transient clouds. It is difficult to see clouds in the 7100 - 9200Å range compared with in the 2.12-μm region, because the atmosphere in the visible range is less transparent. We estimate an upper limit of ∼5% for the influence of transient clouds on the total flux of Titan.

The surface albedos of Titan between 7100 - 9200Å are not very accurately determined in the literature — Anderson et al. (2004) derived the surface albedos of $0.1 \sim 0.3$ near 9300Å using their narrow-band near-IR images. Hirtzig et al. (2005) derived the surface albedos of $0.3 \sim 0.4$ between 8000 and 10000Å from their near-IR spectro-images taken at CFHT. Tomasko et al. (2005) reported reflectivities of $0.16 \sim 0.23$ for 8000−9200Å at the Huygens landing site. McCord et al. (2006) analyzed VIMS data taken from several places and derived a reflectivity of ~ 0.3 near 0.75, 0.85, and 0.95μm where CH_4 absorptions are weak. We adopted a value of 0.3 with reference to that of McCord et al. for the globally averaged surface albedo in our model.

The contribution of the Titan's intensity from the backscatterings of haze particles is estimated to be 81% at 1.08μm according to an analysis of VIMS images by Rodriguez et al. (2006), in which case the intensity contribution from the surface should be minor. The contribution from the backscattering is expected to increase in the 7100−9200Å range compared with that at 1.08μm. We calculate that the surface contribution is less than 10% in the 7100−9200Å range, as discussed in §3.4. Furthermore, our model fits are based on a relative intensity scale; and the intensity ratios between the continuum and absorption features are important.

The retrieved optical properties of haze particles from our inversion program are almost independent from the surface albedo variation between 0.1 and 0.5.

(b) Absorption Coefficients of CH_4 between 7100 and 9200Å

Extensive laboratory observations of the CH_4 bands in the visible range have been reported in the literature (e.g., Lutz and Ramsay, 1972; Lutz et al. 1976; Giver, 1978; Scherer et al. 1984; Borass et al. 1994; Singh and O'Brien, 1995; Tsukamoto and Sasada, 1995; O'Brien and Cao, 2002). These observations needed a very long path-length cell, because the CH_4 bands are weak. The laboratory spectra of the 8900Å bands of CH_4 show numerous cumulative lines at planetary temperatures due to several combination bands as listed in Table II of Boraas et al. (1994), for example. Borass et al. and Tsukamoto and Sasada (1995) were able to resolve CH_4 lines measured at very low temperatures of 15 K and 77 K, respectively, but most of the observed lines have not been assigned. Many lines of these bands have not been resolved; and the possibility of predissociation, which would broaden the lines, has not been investigated. In the ultraviolet and visible range, simple molecules, such as SO_2 (e.g., Freeman et al. 1984), CH (e.g., Kim et al. 1997), etc., show diffuse lines, which are usually originated from high-rotational quantum states undergoing predissociation. We did not consider fluorescent emissions from the CH_4 bands in our model, because of the following reasons — (1) For diffuse lines caused by the predissociation, emissions cannot easily occur because dissociation rates are much higher than emission rates. (2) CH_4 fluorescent emissions from the troposphere and stratosphere of Titan are expected to be negligibly small compared with the strong CH_4 absorption features (e.g., Kim et al. 2000). (3) Laboratory observations of fluorescent emissions of the CH_4 bands have not been reported in literature perhaps due to difficulty in observing weak emissions arising from a long-pathlength cell.

The laboratory spectra presented in the literature have been obtained at several selected temperatures only, not covering the whole temperature range of the Titan's atmosphere. Another difficulty to analyze our high-resolution spectra ($\Delta\lambda \sim 0.27$Å) is the absence of high-resolution laboratory spectra available in the literature. There have been several attempts to observe the CH_4 bands with very high spectral resolving pow-

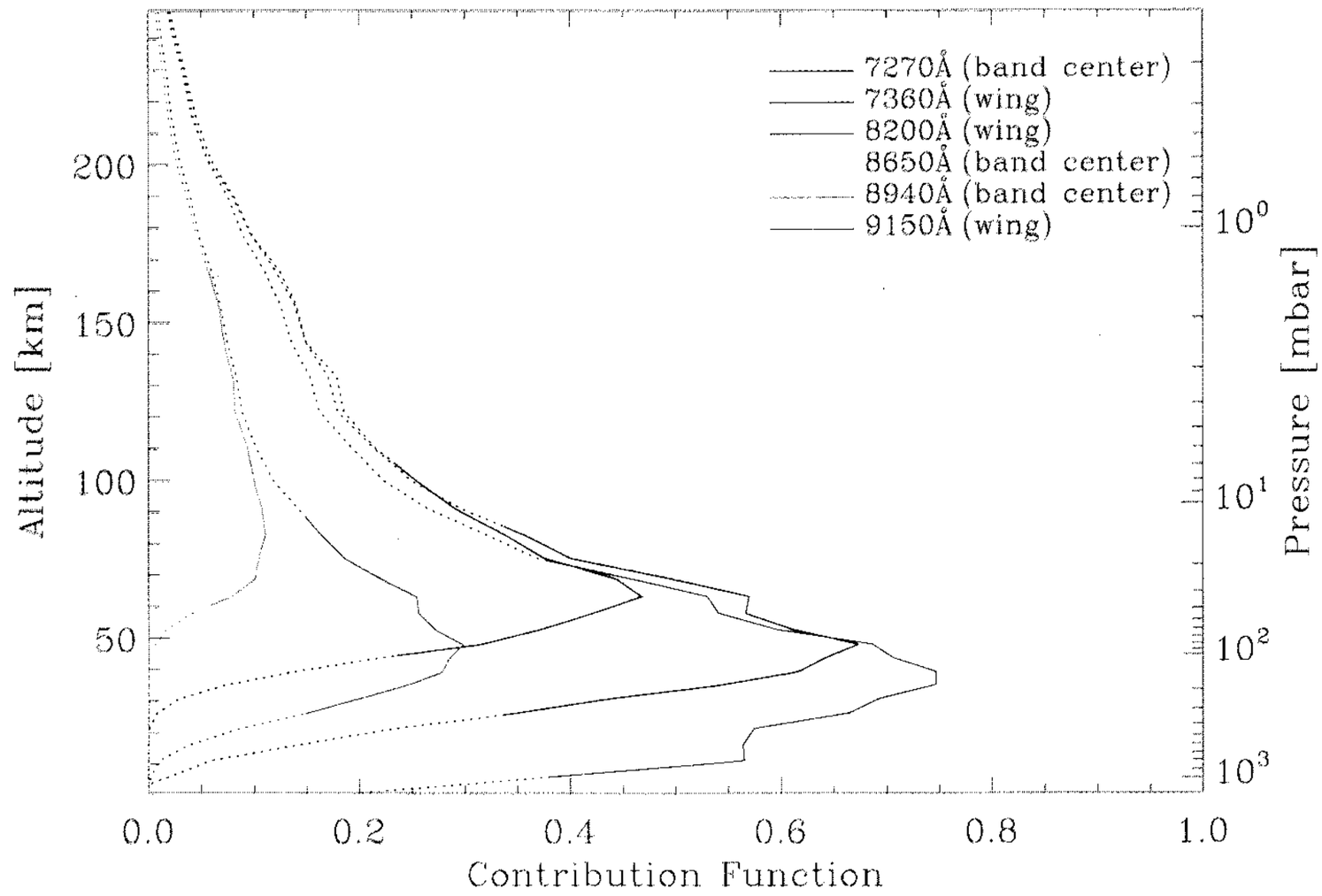

Fig. 3.— Representative contribution functions at 7270 (violet), 7360 (blue), 8200 (green), 8650 (yellow), 8940 (orange), and 9150 (red) Å. The solid or dotted lines represent altitude ranges correspond to within or outside of FWHMs of the contribution functions, respectively.

ers (e.g., $\lambda/\Delta\lambda = 400,000 - 500,000$ of O'Brien and Cao, 2002), but these data are not publically available (O'Brien, private communications, 2007). In this paper, we adopted 1 cm^{-1} ($\sim$0.81Å) resolution absorption coefficients measured at 77 K, which is close to the atmospheric temperatures of Titan, from the tables of Singh and O'Brien (1996) and O'Brien and Cao (2002) for the 7100−7400Å and 8486−9200Å ranges, respectively. Between 7400 and 8486Å, we adopted absorption coefficients with a $\sim$10Å resolution deduced from analyses of planetary spectra by Karkoschka (1994).

The resultant absorption coefficients have been binned with a 20Å box function for the analyses of the smoothed BOES spectrum shown in Fig. 2. Since our major objective of this work is to derive the haze opacities, which should vary with wavelengths smoothly, the binned CH_4 absorption coefficients are proper for our purpose. However, as presented in Fig. 1, the BOES spectrum with a 0.27Å resolution shows many absorption features, which are not very well matched with the 0.81Å resolution CH_4 spectrum, and there might be weak absorption features of other molecules. At the present time, we are unable to confirm that all of these absorption features are due to CH_4 because of lack of high-resolution laboratory spectra of CH_4. In the BOES spectra between 7100 and 9200Å, no significant absorption features of other atmospheric constituents seem to be found, and, therefore, we included only the CH_4 absorption coefficients in the radiative transfer program. Obviously, we need high-resolution laboratory spectra measured at various planetary temperatures for better spectral analyses.

(c) Inversion Program

In order to derive globally averaged haze opacities from the Titan spectra, we have developed an inversion program based on a radiative transfer program described in Kim et al. (2005). The foundation of theoretical formulae has been presented by Banfield et al. (1998) and Stam et al. (2001), who derived vertical distributions of aerosols in the atmospheres of Jupiter and Saturn, respectively, using their inversion

programs. The inversion of planetary spectra has been mainly used for the derivations of temperature-pressure profiles from thermal infrared spectra (e.g., Conrath, 1972; Ohring, 1973; Orton, 1977; and Wallace and Smith, 1979).

In the radiative transfer program, the monochromatic optical depth of a plane-parallel atmospheric layer containing haze, nitrogen molecules, and methane is a combination of those optical depths of the haze, Rayleigh scattering, and methane:

$$\tau_{total} = \tau_{haze} + \tau_{Rayleigh} + \tau_{CH_4} \quad (1)$$

The optical depth of the haze particles in the atmospheric layer is given by,

$$\tau_{haze} = (\kappa_{abs} + \sigma_{scat})dx, \quad (2)$$

where κ_{abs} and σ_{scat} are the absorption and scattering coefficients, respectively, to be determined in a unit of km^{-1}; and dx is the thickness of the plane-parallel layer. The $\kappa_{abs} + \sigma_{scat}$ is designated as "extinction coefficient" in a unit of km^{-1}. The single scattering albedo of the haze particles and the total single scattering albedo are given by

$$\omega_{haze} = \frac{\sigma_{haze}}{(\kappa_{abs} + \sigma_{scat})}, \quad (3)$$

and

$$\omega_{total} = \frac{(\sigma_{scat} + \sigma_{Rayleigh})}{(\kappa_{abs} + \sigma_{scat} + \sigma_{Rayleigh} + \kappa_{CH_4})}, \quad (4)$$

respectively, where $\sigma_{Rayleigh}$ and κ_{CH_4} are the coefficients of Rayleigh scattering and CH_4 absorption, respectively.

The inversion program is designed to determine the wanted parameters, $\kappa_{abs} + \sigma_{scat}$ and ω_{haze}, by means of iterations starting with initial trial parameters so that the synthetic spectrum approaches to the observed spectrum asymptotically. A monochromatic contribution function (Orton, 1977), which is the integrand of the radiative transfer integral, has been revised after each iteration. Since the contribution functions have different altitudinal peaks at different wavelengths, the functions have been used to adjust altitudinally different input parameters after the iterations. We used more than 1100 wavelength points to insure the derived extinction coefficients and single scattering albedos to be constrained. We stopped the iterations when the difference between the model and the observation became less than an observational error bar of 0.005 in the albedo scale in Fig. 2. The retrieved parameters, $\kappa_{abs} + \sigma_{scat}$ and ω_{haze}, from the inversion program should be converged in a bearable number of iterations to be physically meaningful during the iterations. As we mentioned in §3.1, we are unable to derive unique solutions for other quantities, such as the index of refraction, scattering phase function, and size and shape distributions of haze particles, because of excessive number of free parameters to be retrieved.

Even after this simplification, it is not easy to derive unique solutions $\kappa_{abs} + \sigma_{scat}$ and ω_{haze} from the BOES spectrum unless they are tightly constrained. We used intrinsic constraints for τ_{haze} and ω_{haze}, which should vary from 0 to ∞ , and from 0 to 1, respectively. In order to save computer times, we initially tried to derive two quantities for τ_{haze} and ω_{haze}, which are assumed to be correlated with each other, and which should be obtained with a minimum number of the iterations. After we obtained the quantities, we start varying the 2 parameters vertically to determine allowable limits of the parameters. We also initially set the altitudinal variation of τ_{haze} is similar to that of $\sigma_{scat}dx$, since theoretical consideration in the literature (e.g., Young et al. 2002) suggests that ω_{haze} should become less than 0.5 approximately above 150 km, as discussed in §3.4.

In Fig. 3, we present contribution functions, 7270, 7360, 8200, 8650, 8940, and 9150Å among ~1100 data points, for example, with the solid or dotted lines, which are within or outside of the altitude range corresponds to full-width at half-maximum (FWHM) of the contribution functions. As shown in this figure, the peaks of the contributions vary from near the surface to ~90 km, but the influence of the contributions can be up to 250 km. As expected, the peaks corresponding to strong CH_4 absorptions bands at 7270, 8650, and 8940Å occur at higher altitudes than those corresponding to band wings at 7360, 8200, and 9150Å, where CH_4 absorptions are weak.

(d) Properties of Global Haze Particles and Error Analyses

In Fig. 4, we present the retrieved vertical variations of global extinction coefficients, $\kappa_{abs} + \sigma_{scat}$, in a unit of $\log_{10}(km^{-1})$ at 7270, 7360, 8200, 8650, 8940, and 9150Å. It should be noted that although we started with a same initial trial extinction coefficient for all the wavelengths, the retrieved extinction coefficients are different from wavelength to wavelength. In this figure, the solid or dotted lines are the retrieved coefficients for altitude ranges within or outside of the FWHMs (30−120 km) of the contribution functions, respectively. Previous works by Rages and Pollack (1983), McKay et al. (1989), Rannou et al. (1995), Young et al. (2002), and Tomasko et al. (2005) are also presented for comparisons. The thin solid line of Tomasko et al. was derived from an optical-depth curve for 8290Å in Fig. 16b of Tomasko et al. The retrieved solutions (color lines) from the inversion program are closely packed graphically showing the ranges of allowable limits for the coefficients. As suggested by the contribution functions in Fig. 3, the allowable ranges shown in Fig. 4 become widened above the ~150 km altitude, because the contributions of the haze decrease significantly there. Also shown in Fig. 4, the extinc-

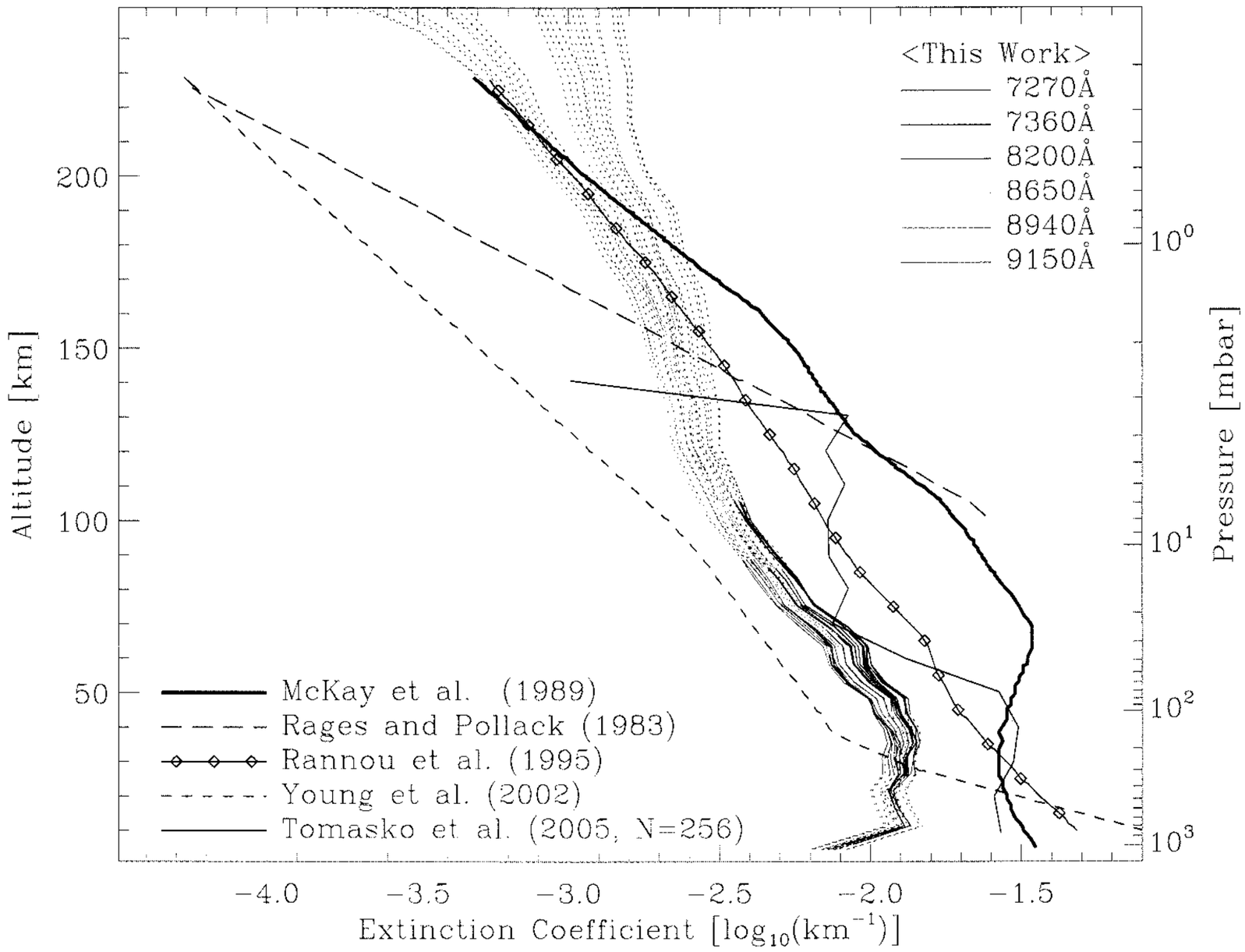

Fig. 4.— The altitudinal variations of the global extinction coefficients, $\kappa_{abs}+\sigma_{scat}$, of haze particles in a unit of $\log_{10}(\mathrm{km}^{-1})$ at 7270 (violet), 7360 (blue), 8200 (green), 8650 (yellow), 8940 (orange), and 9150 (red)Å. The color lines are highly accumulated to show a range of uncertainty in the solutions, which were retrieved from the inversion program. The solid or dotted lines represent altitude ranges correspond to within or outside of FWHMs of the contribution functions, respectively. Detailed structures in the color lines may result from numerical approximations, and may not be physically meaningful.

tion coefficients increase toward the surface. Detailed structures in our model lines may result from numerical approximations, and may not be physically meaningful. It should also be noted that abrupt altitudinal changes less than the FWHM scales cannot be retrieved from our inversion program.

As clearly shown in Fig. 4 with solid color lines is that the extinction coefficients at shorter wavelengths (violet and blue lines) are greater than those at longer wavelengths (orange and red lines) within the FWHMs of the contribution functions, and this trend is not very clear for the outside of the FWHMs, where model uncertainties increase significantly. The accumulative optical depths for 7270−7360Å and 8940−9150Å ranges are estimated to be approximately 1.4 and 1.2, respectively, indicating that the Titanian haze becomes optically thin toward the longer wavelength range. Tomasko et al. (2005) presented total optical depths of 2.5 $\sim$ 3.5 at 8290Å depending on particle aggregation models using Huygens/DISR data. The total optical depths of our results seem to be less than those of Tomasko et al., even after a $\sim$100% systematic error discussed below. At this moment, it is not very clear whether the difference is caused by a local increase of the optical depths at the landing site, or by other reasons. However, if we consider the $\sim$100% error bar, our results are partially overlapped with the results of Tomasko et al.

In Table 1, we listed various sources of uncertainties, which should be added to the extinction coefficients shown in Fig. 4 to be the total error bars of the coefficients. These uncertainties should be systematic errors in the extinction coefficients. The uncertainties related with CH_4, which are marked with in Table 1, are wavelength dependent. In the wavelength ranges where CH_4 absorptions are weak, the effects of the uncertainties in CH_4 absorption coefficients are not significant. There are other uncertainties, not listed in

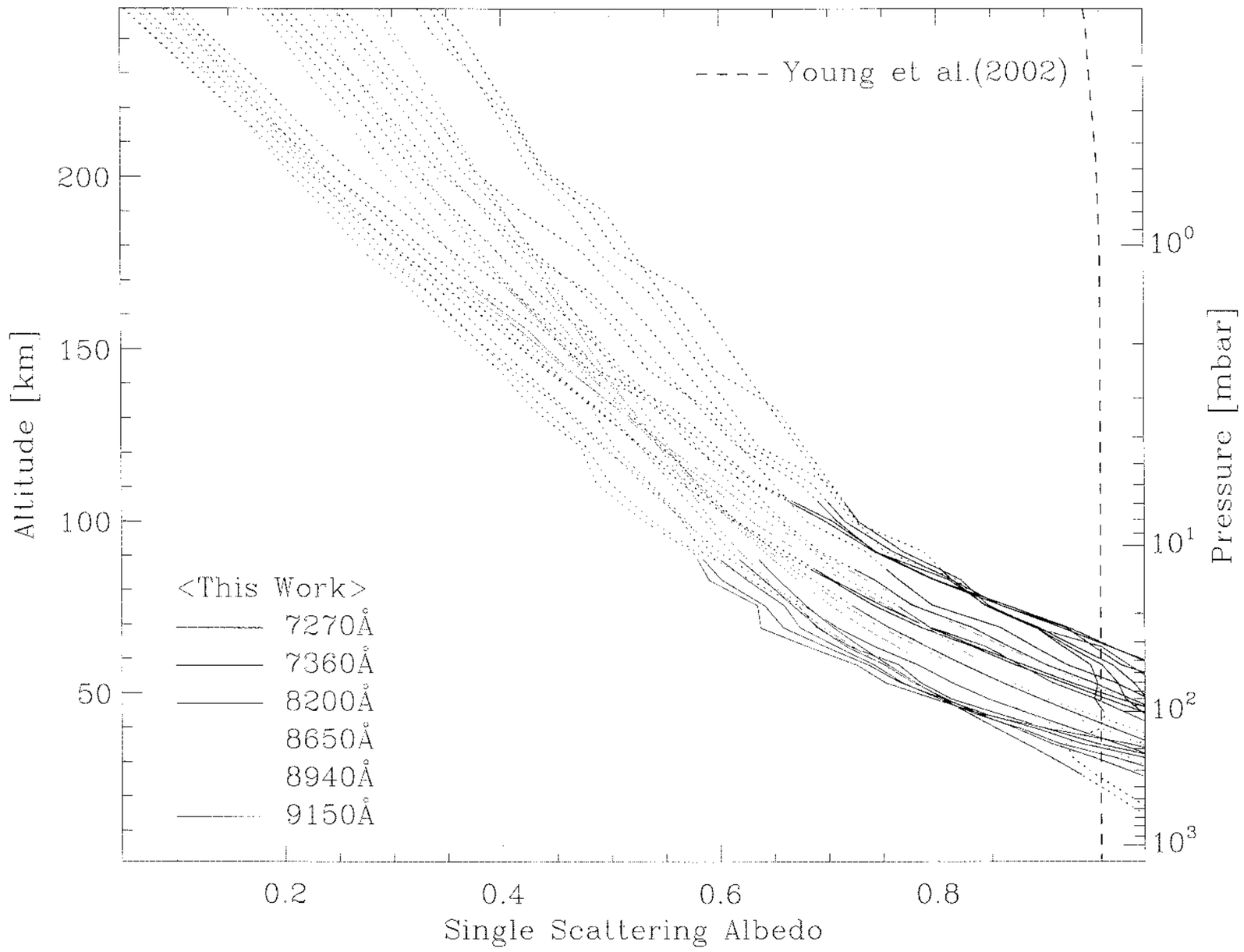

Fig. 5.— Retrieved ω_{haze} haze profiles at 7270 (violet), 7360 (blue), 8200 (green), 8650 (yellow), 8940 (orange), and 9150 (red) Å. A ω_{haze} haze profile of Young et al. (2002) with a dashed black line is presented for a comparison. The width of the solutions can be regarded as the uncertainty of the retrieved ω_{haze} haze profiles. The solid or dotted lines represent altitude ranges correspond to within or outside of the FWHMs of the contribution functions, respectively.

Table 1, such as uncertainties arising from an isotropic and single scattering assumption, and spherical geometry as well as plane-parallel layer approximation. We estimate the uncertainty caused by the spherical geometry and plane-parallel layer approximations should be less than 20% in terms of the extinction coefficients. Regarding the uncertainties arising from the isotropic and single scattering assumptions, we calculated the uncertainties using a program provided by S.S. Hong and H.K. Yang (private communications, 2007). The program is designed to calculate maximum ranges of outgoing radiation from a planet considering extreme cases of multiple scatterings and scattering phase functions using input parameters of the derived total optical depths, 1.2 - 1.4, and single scattering albedos discussed below. We calculated a maximum uncertainty of 31% in terms of resultant intensities. Assuming that all of these uncertainties occur independently, we found that the uncertainty in the possible global variation of CH_4 mixing ratios dominates the total error bar, which is approximately ~100%. Therefore, the ~100% uncertainty should be added to the extinction coefficients shown in Fig. 4 to represent the total error bars at certain altitudes.

In Fig. 5, we present a group of retrieved solutions, which are ω_{haze} profiles with color lines, and a ω_{haze} profile of Young et al. (2002) with a black dashed line for a comparison. Young et al. calculated a theoretical ω_{haze} profile at 8880Å using aggregated particle models; and their ω_{haze} profile is close to 0.95 below 200 km altitude. Their particle models begin as single spherical monomers at 700 km; and as they descend, they form aggregates of two, four, eight, etc., monomers. Since the scattering cross sections increase with size faster than the absorption cross sections do, the single scattering albedos, which are dark at the highest altitudes, eventually become quite bright near the surface. Our result of less bright particles compared with Young et al. below 250 km suggests that the aggregation process during the descent may not be similar to the scenario

TABLE 1.
UNCERTAINTIES IN VARIOUS PARAMETERS, WHICH AFFECT THE ERROR BARS OF THE RETRIEVED PARAMETERS, $\kappa_{abs} + \sigma_{scat}$.

PARAMETER	UNCERTAINTY IN THE PARAMETER (%)	UNCERTAINTY IN $\kappa_{abs} + \sigma_{scat}$ (%)
[1]FULL-DISK ALBEDO VS. GEOMETRIC ALBEDO	0.1	<0.1
[1]SEASONAL VARIATIONS OF TITAN'S BRIGHTNESS	2.4	<2.4
[2]INTENSITY CONTRIBUTION FROM SURFACE	< 10	$3 \sim 4$
[2]INFLUENCE OF TRANSIENT CLOUDS ON TOTAL FLUX	<5	<5
[2]TEMPERATURE DEPENDENCY OF CH_4 ABSORPTION COEFFICIENTS	* <20	* <10
[3]POSSIBLE CH_4 EMISSIONS	* <5	* <3
[4]GLOBAL VARIATION OF CH_4 MIXING RATIO	~200	* ~100
[5]2-STREAM APPROXIMATION	~5	<5
[6]SINGLE SCATTERING APPROXIMATION	< 20	<20

[1] See §2
[2] See §3(a)
[3] See §3(b)
[4] Paulo and Griffith (2006)
[5] Verhoef (1988)
[6] Kim et al. (2005)
* Wavelength dependent
See §3(e) for other uncertainties, not listed in Table 1, such as uncertainties arising from an isotropic and single scattering assumption, a numerical approximation of spherical geometry, and a plane-parallel layer approximation.

of Young et al.

The wavelength-dependent pattern of the ω_{haze} profiles in Fig. 5 is similar to that of the extinction coefficients shown in Fig. 4 — The ω_{haze} at shorter wavelengths (blue and violet lines) are greater than the ω_{haze} at longer wavelengths (yellow and orange lines) within the FWHMs. The both quantities increase toward the surface, otherwise the number of the iterations of the inversion computations increases and the parameters could not be converged easily. The retrieved ω_{haze} profiles approach to 1.0 toward the surface, and they are less than 0.5 at altitudes higher than ~150 km. The vertical variations suggest the following properties of the haze particles for the 7100−9200Å range — Near the surface, the scattering coefficients, σ_{scat}, are greater than the absorption coefficients, κ_{abs}, and the sizes of the haze particles are comparable to or greater than the wavelengths. At altitudes above the ~150 km level, σ_{scat} becomes less than κ_{abs}, suggesting that the particle sizes are likely to be smaller than the wavelengths.

In §3.1, we mentioned that Rodriguez et al. (2006) estimated that the contribution of the Titan's intensity from the backscattering of haze particles is 81% at 1.08 m and the contribution from the surface should be minor. Fig. 5 demonstrates that the scatterings of the haze particles are indeed significant especially near the surface. We estimate that the contribution from the surface to the total intensity is less than 10%, and that the scatterings of the haze particles dominate the brightness of Titan in the 7100−9200Å range.

IV. CONCLUSIONS

We have derived globally averaged optical properties of Titan's haze particles from visible spectra between 7100 and 9200Å, which were obtained with an echelle spectrograph (BOES) at Bohyunsan Observatory in Korea. Since the observations were carried out near the activities of the Cassini T3 and Huygens observations of Titan, our results are complementary to the historic results of this mission. In order to derive the extinction coefficients and single scattering albedos of haze particles, we developed an inversion radiative-transfer program using an atmospheric model of Titan and laboratory CH_4 absorption coefficients available in the literature. It is obvious that we need high-resolution laboratory CH_4 spectra measured at the atmospheric temperatures of Titan in order to accurately model the Titan spectra.

The derived extinction coefficients of the haze increase toward the surface, and the coefficients at shorter wavelengths are greater than those at longer wavelengths for the 30−120 km altitude range. Total accumulative optical depths for 7270−7360Å and 8940−9150Å ranges are estimated to be 1.4 and 1.2, respectively, indicating that the Titanian haze becomes optically thin toward the longer wavelength range. Tomasko et al. (2005) presented total optical depths of

$2.5 \sim 3.5$ at 8290Å depending on particle aggregation models using Huygens/DISR data. The total optical depths of our results seem to be less than the results of Tomasko et al. However, our results are partially overlapped with the range of the results of Tomasko et al. considering the ~100% error bar, which was calculated from extensive error analyses presented in the main text.

The derived single scattering albedos of the haze particles approach to 1.0 toward the surface, and they are less than 0.5 at altitudes higher than ~150 km, suggesting that near the surface, the haze particle sizes are comparable to or greater than the wavelengths, and at altitudes above ~150 km level, the particle sizes become smaller than the wavelengths. We also found that the scatterings of the haze particles dominate the brightness of Titan in the 7100−9200Å range, and intensity contributions from the surface to the total intensity is less than 10%, which is consistent with a result of Rodriguez et al. (2006).

ACKNOWLEDGEMENTS

We would appreciate useful discussions with Dr. O'Brien for the availability of high-resolution laboratory spectra of CH_4. NSO/Kitt Peak FTS data used here were produced by NSF/NOAO. This research has been partially supported by a research grant of Kyung Hee University.

REFERENCES

Anderson, C. M., Chanover, N. J., McKay, C. P., Rannou, P., Glenar, D. A., & Hillman, J. J., 2004, Titan's haze structure in 1999 from spatially-resolved narrowband imaging surrounding the 0.94μm methane window, Geophys. Res. Lett., 31, L17S06

Banfield, D., Conrath, B. J., Gierasch, P. J., & Nicholson, P. D., 1998, Near-IR Spectrophotometry of Jovian Aerosols-Meridional and Vertical Distributions, Icarus, 134, 11

Boraas, K., Lin, Z., & Reilly, J. P., 1994, High resolution study of methane's $3\nu_1+\nu_3$ vibrational overtone band, J. Chem. Phys., 100, 7916

Bowles, N., Barnett, J .J., Smith, K., Williams, G., & Calcutt, S., 2006, Visible and Near-infrared Spectroscopy (0.6 to 1.1μm) of Methane Gas to Support Remote Sensing of Outer Planet Atmospheres. 38th DPS Meeting, #62.15, Bull. Amer. Astron. Soc., 38, 608

Chamberlain, J. W. & Hunten, D., 1987, Theory of Planetary Atmospheres, An Introduction to Their Physics and Chemistry, New York: Academic

Conrath, B. J., 1972, Vertical Resolution of Temperature Profiles Obtained from Remote Radiation Measurements, J. Atm. Sci., 29, 1262

Coustenis, A., Lellouch, E., Maillard, J. P., & McKay, C. P., 1995, Titan's Surface: Composition and Variability from the Near-Infrared Albedo, Icarus, 118, 87

Flasar, F. M., Samuelson, R. E., & Conrath, B. J., 1981, Titan's atmosphere: temperature and dynamics, Nature, 292, 693

Freeman, D. E., Yoshino, K., Esmond, J. R., & Parkinson, W. H., 1984, High resolution absorption cross section measurements of SO_2 at 213 K in the wavelength region 172-240 nm, Planet. Space Sci., 32, 1125

Fulchignoni, M.,et al., 2005, In situ measurements of the physical characteristics of Titan's environment, Nature, 438, 785

Gendron, E., et al., 2005, On an ESO website: http://www.eso.org/outreach/press-rel/pr2005/phot-04-05.html#note1

Giver, L. P., 1978, Intensity measurements of the CH_4 bands in the region 4350Å to 10,600Å, J. Quant. Spectrosc. Radiat. Trans, 19, 311

Griffith, C. A., Owen, T., & Wagener, R., 1991, Titan's Surface and Troposphere, Investigated with Ground-Based, Near-Infrared Observations, Icarus, 93, 362

Griffith, C. A., Owen, T., Miller, G. A., & Geballe, T., 1998, Transient clouds in Titan's lower atmosphere, Nature, 395, 575

Griffith, C.A ., Owen, T., Geballe, T. R., Rayner, J., & Rannou, P., 2003, Evidence for the Exposure of Water Ice on Titan's Surface, Science, 300, 628

Hall, J. C., Fulton, E. E., Huenemoerder, D. P., Welty, A. D., & Neff, J. E., 1994, The reduction of fiber-fed echelle spectrograph data: Methods and an IDL-based solution procedure, Astron. Soc. Pacific, 106, 315

Harri, A.-M., Mäkinen, T., Lehto, A., Kahanpää, H., & Siili, T., 2006, Vertical pressure profile of Titan-observations of the PPI/HASI instrument, Planet. Space Sci., 54, 1117

Hinkle, K., Wallace, L., Livingston, W., Ayres, T., Harmer, D., & Valenti, V., 2003, High Resolution Infrared, Visible, and Ultraviolet Spectral Atlases of the Sun and Arcturus. Proceedings of 12th Cambridge Workshop on Cool Stars, Stellar Systems, & The Sun, 2003 University of Colorado, 851

Hirtzig, M., Coustenis, A., Lai, O., Emsellem, E., Pecontal-Rousset, A., Rannou, P., Negrão, A., & Schmitt, B., 2005, Near-infrared study of Titan's resolved disk in spectro-imaging with CFHT/OASIS, Planet. Space Sci, 53, 535

Karkoschka, E., 1994, Spectrophotometry of the Jovian Planets and Titan at 300- to 1000-nm Wavelength: The Methane Spectrum, Icarus, 111, 174

Karkoschka, E., 1998, Methane, Ammonia, and Temperature Measurements of the Jovian Planets and Titan from CCD-Spectrophotometry, Icarus, 133, 134

Kim, S. J., Brown, M., & Spinrad, H., 1997, High-resolution spectroscopy of the A-X and B-X systems of CH in comets, J. Geomagnet. Geoelectr, 49, 132

Kim, S. J., Geballe, T. R., & Noll, K.,S., 2000, NOTE: Three-Micrometer CH_4 Line Emission from Titan's High-Altitude Atmosphere, Icarus 147, 588

Kim, S. J., Geballe, T. R., Noll, K. S., & Courtin, R., 2005, Clouds, haze, and CH_4, CH_3D, HCN, and C_2H_2 in the atmosphere of Titan probed via 3μm spectroscopy, Icarus, 173, 522

Lindal, G. F., Wood, G. E., Hotz, H. B., Sweetnam, D. N., Eshelman, V. R., & Tyler, G. L., 1983, The atmosphere of Titan: An analysis of the Voyager 1 radio-occultation measurements, Icarus, 53, 348

Lorenz, R. D., Lemmon, M. T., Smith, P. H., & Lockwood, G. W., 1999, Seasonal change on Titan observed with the Hubble Space Telescope WFPC-2, Icarus, 142, 391

Lutz, B. L. & Ramsay, D. A., 1972, New observations on the Kuiper bands of Uranus, Astrophys. J., 176, 521

Lutz, B. L., Owen, T., & Cess, R. D., 1976, Laboratory band strengths of methane and their application to the atmospheres of Jupiter, Saturn, Uranus, Neptune, and Titan, Astrophys. J., 203, 541

McCord, T. B., the Cassini VIMS Team, et al., 2006, Composition of Titan's surface from Cassini VIMS, Planet. Space Sci., 54, 1524

McKay, C. P., Pollack, J.B ., & Courtin, R., 1989, The Thermal Structure of Titan's Atmosphere, Icarus, 80, 23

Neff, J. S., Humm, D. C., Bergstralh, J. T., Cochran, A. L., Cochran, W. D., Barker, E. S., & Tull, R. G., 1984, Absolute Spectrophotometry of Titan, Uranus, and Neptune: 3500-10,500Å, Icarus, 60, 221

Negrão, A., Coustenis, A., Lellouch, E., Maillard, J.-P., Rannou, P., Schmitt, B., McKay, C. P., & Boudon, V., 2006, Titan's surface albedo variations over a Titan season from near-infrared CFHT/FTS spectra, Planet. Space Sci., 54, 1225

Niemann, H. B., et al., 2005, The abundances of constituents of Titan's atmosphere from the GCMS instrument on the Huygens probe, Nature, 438, 779

O'Brien, J. J. & Cao, H., 2002, Absorption spectra and absorption coefficients for methane in the 750-940nm region obtained by intracavity laser spectroscopy, J. Quant. Spectrosc. Rad. Transf, 75, 323

Ohring, G., 1973, The Temperature and Ammonia Profiles in the Jovian Atmospheres from Inversion of the Jovian Emission Spectrum, Astrophys. J., 184, 1027

Orton, G. S., 1977, Recovery of the mean Jovian temperature structure from inversion of spectrally resolved thermal radiance data, Icarus, 32, 41

Paulo, P. F., Griffith, C., & the Cassini VIMS team, 2006, Constraints on the variability of the tropospheric methane abundance on Titan from Cassini VIMS observations, 38th DPS Meeting, #27.16, Bull. Amer. Astron. Soc., 38, 530

Rages, K., & Pollack, J. B., 1983, Vertical Distribution of Scattering Hazes in Titan's Upper Atmosphere, Icarus, 55, 50

Rannou, P., Cabane, M., Chassefiere, E., Botet, R., McKay, C. P., & Courtin, R., 1995, Titan's geometric albedo: Role of the fractal structure of the aerosols, Icarus, 118, 355

Rodriguez, S., Le Mouélic, S., Sotin, C., Clénet, H., Clark, R. N., Buratti, B., Brown, R. H., McCord, T. B., Nicholson, P. D., Baines, K. H., & the VIMS Science Team, 2006, Cassini/VIMS hyperspectral observations of the HUYGENS landing site on Titan, Planet. Space Sci., 54, 1510

Scherer, G. J., Lehmann, K. K., & Klemperer, W., 1984, The high-resolution visible overtone spectrum of CH_4 and CD_3H at 77 K, J. Chem. Phys., 81, 5319

Škoda, P. & Hensberge, H., 2003, Merging of Spectral Orders from Fiber Echelle Spectrographs, ASP Conference Series, 295, 415

Singh, K. & O'Brien, J. J., 1995, Laboratory measurements of absorption coefficients for the 727-nm band of methane at 77 K and comparison with results derived from spectra of the giant planets, J. Quant. Spectrosc. Radiat. Trans., 54, 607-619

Smith, P. H., Lemmon, M. T., Lorenz, R. D., Sromovsky, L. A., Caldwell, J. J., & Allison, M. D., 1996, Titan's Surface, Revealed by HST Imaging, Icarus ,119, 336

Stam, D. M., Banfield, D., Gierasch, P. J., Nicholson, P. D., & Matthews, K., 2001, Near-IR Spectrophotometry of Saturnian Aerosols-Meridional and Vertical Distribution, Icarus, 152, 407

Tomasko, M. G., et al., 2005, Rain, Winds and haze during the Huygens probe's descent to Titan's surface, Nature, 438, 765

Tsukamoto, T. & Sasada, H., 1995, Extended assignments of the $3\nu_1+\nu_3$ band of methane, J. Chem. Phys., 102, 5126

Wallace, L. & Smith, G. R., 1979, The Jovian temperature structure obtained by inversion of infrared spectral measurements, Icarus, 38, 342

Young, E. F., Rannou, P., McKay, C. P., Griffith, C. A. &, Noll, K., 2002, A three-dimensional map of Titan's tropospheric haze distribution based on Hubble Space Telescope imaging, Astron. J., 123, 3473